Origin of Coexisting Minette and Ultramafic Breccia, Navajo Volcanic Field

Michael F. Roden

Center for Geoalchemy, Department of Earth and Planetary Sciences, Massachusetts Institute of Technology, Cambridge, Massachusetts 02139, USA

Abstract. Trace element evidence indicates that at the Buell Park diatreme, Navajo volcanic field, the felsic minette can be best explained by crystal fractionation from a potassic magma similar in composition to the mafic minettes. Compatible trace element (Cr, Ni, Sc) abundances decrease while concentrations of most incompatible elements (Ce, Yb, Rb, Ba, Sr) remain constant or increase from mafic to felsic minette. In particular, the nearly constant Ce/Yb ratio of the minettes combined with the decrease in Cr, Ni, and Sc abundances from mafic to felsic minette is inconsistent with a model of varying amounts of partial melting as the process to explain minette compositions. The uniformity of rare earth element (REE) abundances in all the minettes requires that an accessory mineral, apatite, dominated the geochemistry of the REE during fractionation. A decrease in P_2O_5 from mafic to felsic minette and the presence of apatite in cognate inclusions are also consistent with apatite fractionation. Higher initial $^{87}Sr/^{86}Sr$ ratios in the felsic minettes relative to the proposed parental mafic minettes, however, is inconsistent with a simple fractionation model. Also, a separated phlogopite has a higher initial $^{87}Sr/^{86}Sr$ ratio than host minette. These anomalous isotopic features probably reflect interaction of minette magma with crust.

The associated ultramafic breccia at Buell Park is one of the Navajo kimberlites, but REE concentrations of the matrix do not support the kimberlite classification. Although the matrix of the breccia is enriched in the light REE relative to chondrites, and has high La, Rb, Ba, and Sr concentrations relative to peridotites, the concentrations of these elements are significantly lower than in South African kimberlites. A high initial $^{87}Sr/^{86}Sr$ ratio combined with petrographic evidence of ubiquitous crustal xenoliths in the Navajo kimberlites suggests that the relatively high incompatible element concentrations are due to a crustal component. Apparently, Navajo kimberlites are most likely a mixture of comminuted mantle wall rock and crustal material; there is no evidence for an incompatible element-rich magma which is characteristic of South African kimberlites.

If the mafic minettes are primary magmas derived from a garnet peridotite source with chondritic REE abundances, then REE geochemistry requires very small (less than 1%) degrees of melting to explain the minettes. Alternatively, the minettes could have formed by a larger degree of melting of a metasomatized, relatively light REE-enriched garnet peridotite. The important role of phlogopite and apatite in the differentiation of the minettes supports this latter hypothesis.

Introduction

Volcanic rocks of the ultrapotassic series (Carmichael et al. 1974) are rare lavas characterized by trace element geochemistry similar to that of kimberlites. For example, more mafic compositions have high concentrations of the compatible elements such as Mg, Ni, and Cr, but also have $K_2O/Na_2O > 1$ and high concentrations of incompatible elements such as La, Rb, and Ba. Kay and Gast (1973) summarized rare earth element (REE) abundance data that suggested these lavas formed by small amounts of partial melting of garnet peridotite in the upper mantle.

The Oligocene minettes of the Navajo volcanic field (Fig. 1; Williams 1936) belong to the ultrapotassic series. Petrographically, they are characterized by phenocrysts of phlogopite + diopside ± olivine in a groundmass of phlogopite, diopside, sanidine, apatite, and oxides. Spinel peridotite xenoliths are widely distributed; garnet peridotite xenoliths are less common (Ehrenberg 1979). Typical Navajo minettes have high MgO concentrations (4.3 to 13.3 wt. % Ehrenberg 1977; Nicholls 1969; Roden and Smith 1979; Williams 1936), high Cr and Ni concentrations (95 to 631 ppm and 123 to 481 ppm respectively, Ehrenberg 1977; Nicholls 1969; this paper), large La/Yb ratios relative to chondrites (Kay and Gast 1973; Ehrenberg 1977; this paper), and relatively high initial $^{87}Sr/^{86}Sr$ ratios for mantle-derived magmas (0.705 to 0.708, Powell and Bell 1970). Most of the Navajo minettes are relatively mafic (48 to 52 wt. % SiO_2) and occur as dikes and diatremes, but in some larger volcanic centers, felsic minette with up to 60 wt. % SiO_2 is associated with mafic minette. Initially, Kay and Gast (1973) suggested mafic and felsic minettes originated as immiscible liquids. Later, Ehrenberg (1977) suggested that at the Washington Pass, Sonsela Buttes, and Mitten Rock centers, the felsic minettes were in part differentiates of the more mafic minettes. Roden and Smith (1979) concluded, however, that the felsic minettes may have formed by smaller degrees of melting than the mafic minettes based on studies of whole rock and phenocryst compositions of minettes from the Buell Park volcanic center. To further evaluate these hypotheses for the relation of felsic to mafic minette, a suite of minettes plus a phlogopite phenocryst separate from Buell Park were analyzed for trace elements and $^{87}Sr/^{86}Sr$ ratios. On the basis of the occurrence of peridotite xenoliths and forsteritic olivine phenocrysts, the Navajo minettes appear to have originated by partial melting in the mantle; thus detailed studies of these volcanic rocks have important implications for the petrogenesis of potassic basalts.

Table 1. Representative minette analyses[a]

Sample	BPR-5	BP-37	BP-35
SiO_2	48.94	56.23	59.50
TiO_2	2.03	1.08	0.89
Al_2O_3	10.11	12.14	12.93
Fe_2O_3	4.47	4.38	3.02
FeO	3.60	1.36	1.46
MnO	0.12	0.08	0.06
MgO	10.03	6.63	4.90
CaO	8.98	6.37	5.30
Na_2O	1.28	2.60	2.53
K_2O	5.22	6.76	7.21
H_2O+	2.92	0.84	0.54
H_2O-	0.80	0.36	0.60
P_2O_5	1.08	0.77	0.64
CO_2	0.01	0.02	0.10
Total	99.59	99.62	99.68
$Mg/Mg+Fe^{2+}$ [b]	72.3	71.2	69.8

[a] Analyses from Roden and Smith (1979)
[b] Assuming Fe^{2+} is 90% of total Fe

Fig. 1. Sketch maps of the Navajo volcanic field (adapted from Smith and Levy 1976) and Buell Park (*inset*). *Filled circles* are minette diatremes and *triangles* are kimberlite pipes. Major monoclines are also shown. Localities mentioned in the text are indicated as follows: *BP*, Buell Park; *MR*, Mitten Rock; *SR*, Shiprock; *TT*, The Thumb; *SB*, Sonsela Buttes; *WP*, Washington Pass; *GN*, Green Knobs; *DB*, Dike B. In the Buell Park sketch map *shaded areas* represent minette and sample localities are indicated by *filled circles*. Abbreviations are as follows: *BM*, Buell Mountain; *UM*, lowland underlain by kimberlite; *UMa*, knob of resistant kimberlite; *RD*, ring dike

Knowledge of compatible and incompatible trace element concentrations in a suite of related volcanic rocks can provide evidence to distinguish between varying amounts of partial melting versus fractional crystallization as the dominant petrogenetic process (see Allegre and Minster 1978) involved in the genesis of the rocks. For example, rocks related by varying amounts of partial melting should have similar compatible element concentrations but quite variable incompatible element concentrations. In contrast, a signature of fractional crystallization is strong depletion in compatible elements accompanied by enrichment of incompatible elements in the differentiated rocks. With these principles in mind, the Buell Park minettes were analyzed for a series of trace elements ranging from compatible (Cr, Ni, Sc) to incompatible (Ba, La, Rb) to determine rock interrelationships.

In addition to the minettes, a sample of the matrix of a kimberlitic tuff from Buell Park was analyzed for trace elements and $^{87}Sr/^{86}Sr$ ratio. These kimberlitic tuffs occur as isolated diatremes along the Monument Uplift (McGetchin and Silver 1972) and in diatremes associated with minette in and near Buell Park. Fission track ages of minerals from inclusions in kimberlitic tuff (Naeser 1971) and field evidence from Buell Park (Roden and Smith 1979) established that minette and kimberlite eruptions were essentially contemporaneous. Relative to South African kimberlites, these tuffs lack the minerals such as phlogopite and perovskite which are rich in incompatible elements (Smith and Levy 1976), and there is no evidence that a true magma was ever associated with these tuffs (McGetchin and Silver 1972).

Field and Sample Description

Details of the field geology and petrology of the minettes and kimberlite from Buell Park were presented by Roden and Smith (1979) and Schmitt et al. (1974). Representative whole rock analyses of Buell Park minettes are presented in Table 1; sample localities are shown in Fig. 1. Buell Park (Fig. 1) is a large circular depression, 4.5 km in diameter, floored by kimberlitic tuff. In the north central region, kimberlitic tuff is intruded by a mass of felsic minette (60 wt. % SiO_2, 5 wt. % MgO) and minette tuff breccia. There is evidence there that minette and kimberlite eruptions overlapped in time: subrounded minette clasts occur in the upper 75 m of layered kimberlitic tuff. Two km southeast
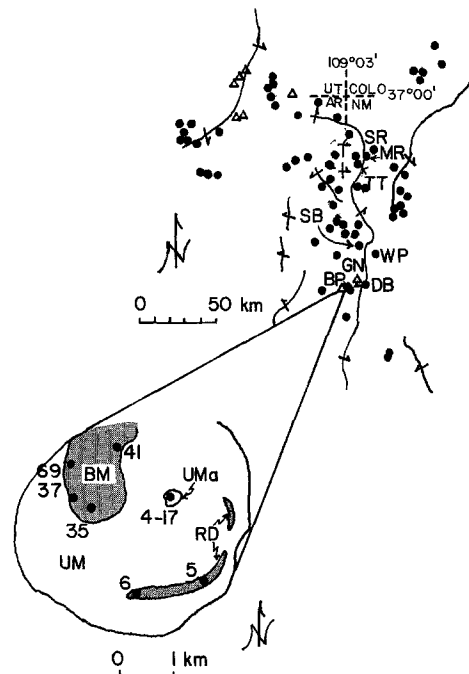
of this mass of felsic minette, a ring dike or cone sheet of mafic minette (49 wt. % SiO_2, 10 wt. % MgO) intruded kimberlitic tuff and now forms a curving ridge. The mafic minettes contain phenocrysts of olivine, diopside, and phlogopite in a matrix of the same plus sanidine, analcime, and oxides. In contrast, the felsic minettes lack olivine and analcime, are lower in MgO and higher in K_2O and SiO_2, and are silica saturated or oversaturated. Only the felsic minettes contain abundant xenoliths and xenocrysts. Descriptions of individual samples are contained in the appendix.

Analytical Data

All samples analyzed were whole rock powders, except kimberlitic tuff NBP4–17 from which matrix material was hand-picked from the 6 to 18 mesh fraction, and BP-37 Mica which was separated by standard mineral separation procedures and then hand-picked to remove impurities. The purity of the mica separate is estimated at >99%, the dominant impurities are pyroxene phenocrysts and groundmass. The data show that the Buell Park minettes are geochemically similar to other rocks of the ultrapotassic series (Table 2, Figs. 2, 3); for example, they have highly fractionated REE patterns relative to chondrites, they contain large amounts of Ba, Rb, and Sr, and they have high Cr and Ni contents. In detail, there are several significant trends: (1) although the REE are highly fractionated, the concentrations of the REE and the Ce/Yb ratio remain relatively constant over the range of MgO present (Figs. 2, 3); (2) the compatible elements Cr, Ni, and Sc decrease rapidly with decreasing MgO (Fig. 3); and (3) elements normally considered incompatible do
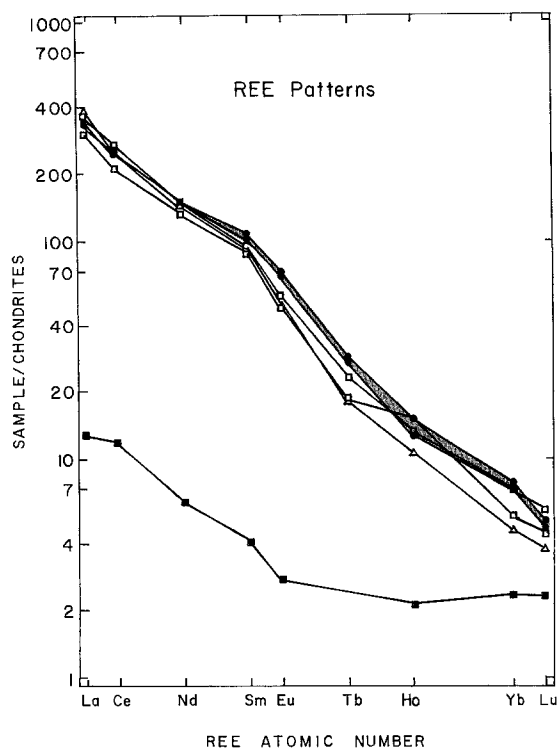
Fig. 2. Chondrite normalized (chondritic concentrations from Frey et al. 1968) REE patterns for Buell Park minettes and kimberlitic tuff. Symbols are as follows: (●) ring dike samples, BPR-5, BPR-6; (□) BP-37; (□) BP-35; (△) minette clast BP-69 from kimberlitic tuff; (■) kimberlitic tuff NBP 4-17. REE Patterns of the two ring dike samples bound the *shaded area*. Sample BP-41 was not plotted to improve clarity

Fig. 3. MgO variation diagrams for trace elements in Buell Park minettes: (●), BPR-5, BPR-6; (○), BP-37: (△), BP-35; (□), BP-41. Sample BP-69 is not plotted on this diagram; the anomalous chemistry of this sample was discussed elsewhere (Roden and Smith 1979)

not behave as a coherent group (Table 2; Fig. 3). For example, with decreasing MgO, Rb and Th increase, Ba and Sr remain essentially constant, and Nb and Ta decrease (Fig. 3; Table 2). The ring dike samples, BPR-5 and BPR-6, are essentially identical in major elements, except for Na_2O (Roden and Smith 1979) and in trace elements except for Rb, Cs, and Sr (Table 2).

The minettes are heterogeneous with respect to $^{87}Sr/^{86}Sr$ ratios (all ratios are age corrected to 25.3 m.y. B.P., see Roden et al. 1979; $\lambda = 1.42 \times 10^{-11}$ yr^{-1}): BPR-6 has a slightly but significantly higher calculated initial $^{87}Sr/^{86}Sr$ ratio than BPR-5 (0.70582 versus 0.70551), and the two felsic minettes, BP-37 and BP-35, from Buell Mountain are both enriched in ^{87}Sr relative to the ring dike minette. Surprisingly, BP-37 Mica has a higher calculated initial $^{87}Sr/^{86}Sr$ ratio than the host rock BP-37.

Relative to the minettes, the kimberlitic tuff is depleted in incompatible elements and enriched in Cr. The REE in the tuff are fractionated ($Ce/Yb_n = 4$ where Ce/Yb_n is the chondrite-normalized ratio) but not so highly fractionated as in the minettes ($Ce/Yb_n = 36$ to 62) and REE concentrations are much lower in the kimberlitic tuff than in the minettes (Fig. 2). The calculated initial $^{87}Sr/^{86}Sr$ ratio of the tuff is substantially higher than that of the minettes (Table 2).

Discussion

1. Potassic Nature of the Primary Navajo Magma

The presence of abundant peridotite xenoliths derived from the upper mantle in some Navajo minettes (Ehrenberg 1979, Roden and Smith 1979) indicates a mantle source for the minettes.
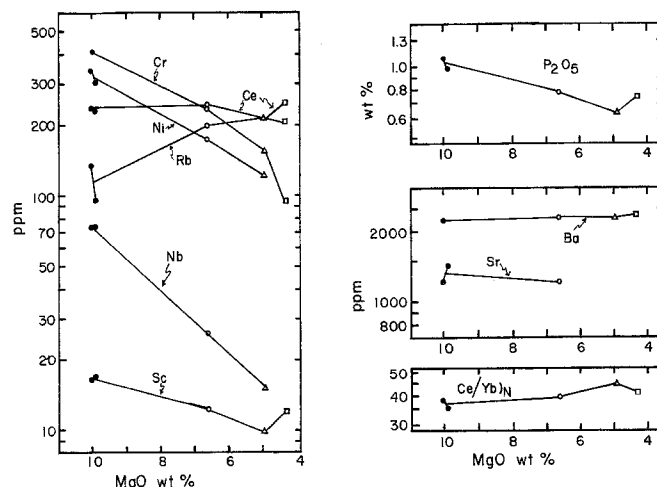
Recent workers in the Navajo field (e.g. Ehrenberg 1977; Roden and Smith 1979) argued that the potassic nature of the minettes reflects partial melting of a portion of the mantle enriched in K and Rb. However, crustal assimilation has also been invoked to explain potassic magmas (see discussion in Bell and Powell 1969); specifically in the case of the Navajo field, Williams (1936) suggested that the minettes formed by reaction of Hopi Buttes monchiquite with granitic xenoliths. A subsequent geochronologic investigation by Naeser (1971) showed that this latter hypothesis was untenable because the Navajo lavas predated the Hopi lavas by more than 20 m.y.

The most mafic Navajo minettes have geochemical and mineralogical characteristics consistent with equilibration with olivine whose composition lies within the range hypothesized for mantle olivine. Potassium content increases somewhat with decreasing MgO in the Navajo lavas, but the K_2O/Na_2O ratio is essentially independent of MgO content, and the most mafic minettes retain the high K_2O/Na_2O ratio characteristic of the minettes in general (Fig. 4). The two most MgO-rich lavas in Fig. 4, Dike B in Todilto Park (Williams 1936) and the Thumb (Ehrenberg 1977) have $Mg/Mg + Fe^{2+}$ (assuming $Fe^{2+} = 0.9$ total Fe) ratios of 77 and 78; melts with these ratios would be in equilibrium with an olivine of composition Fo_{93} (Roeder and Emslie 1970). Such an olivine composition lies within the range suggested for mantle olivine (e.g. Clarke and O'Hara 1979) but is somewhat more Mg-rich than olivines reported in peridotite nodules from the Green Knobs diatreme (Smith and Levy 1976). This difference could be due to a vertical compositional gradient in the mantle but is more likely due to the approximation used to estimate Fe^{2+} or the presence of some cumulate or xenocrystal olivine in these rocks. A dike near Dike B in Todilto Park contains olivine phenocrysts zoned from Fo_{91} (core) to Fo_{87} (rim), thus substantiating the above calculations (Roden and Smith 1979). Thus, the evidence suggests that the primary magma in the Navajo field was potassic and similar in composition to that of The Thumb and Dike B.

2. Relation of Minette Compositional Types: Trace Element Evidence

The occurrence of dense inclusions in the felsic minettes and the absence or scarcity of xenoliths in the associated mafic min-

Table 2. Trace element and Sr isotopic analyses

A. Analyses by instrumental neutron activation (ppm)[a]

Sample	BPR-5	BPR-6	BP-37	BP-35	BP-41	BP-69	NBP4-17
La	116	117	123	109	123	129	4.4
Ce	238	234	243	211	247	248	10
Nd	99	98	99	83	100	97	3.8
Sm	18.2	18.8	17.3	15.6	17.7	15.8	0.78
Eu	4.66	4.83	3.96	3.45	3.91	3.58	0.19
Tb	1.3	1.4	1.2	0.92	1.1	0.89	
Ho	0.91	1.0	0.93	1.1	1.2	0.74	0.2
Yb	1.42	1.49	1.40	1.06	1.38	0.91	0.47
Lu	0.16	0.17	0.19	0.15	0.16	0.13	0.08
Rb	134	96	200	214	207	183	
Ba	2,220	2,110	2,270	2,280	2,350	2,300	293
Th	22.2	22.8	43.0	46.8	45.2	49.4	
Sc	16	17	12	9.8	12	8.7	6.1
Cr	414	410	234	154	95	141	1,770
Ta	3.7	3.7	1.6	1.1	1.2	1.2	

B. Analyses by X-ray fluorescence (ppm)[b]

Sample	BPR-5	BPR-6	BP-37	BP-35	BP-69
Ni	338	305	176	123	270
V	195	189	132	100	96
Zn	92	89	82	74	59
Cu	64	69	96	22	69
Nb	74	74	26	15	24

C. Analyses by mass spectrometry (ppm)[c]

Sample	BPR-5	BPR-6	BP-37	BP-35	NBP4-17	BP-37 Mica
Rb	122	94	206		2.31	394
Cs	2.74	4.8	4.92			
Ba	2,040	2,045	2,375			
Sr	1,256	1,420	1,209		96.2	94.8
$^{87}Sr/^{86}Sr_m$[d]	0.70561 ± 6	0.70589 ± 4	0.70702 ± 7	0.70704 ± 6	0.71191 ± 6	0.71226 ± 4
$^{87}Sr/^{86}Sr_i$[e]	0.70551	0.70582	0.70685		0.71189	0.70804

[a] M.I.T. lab, replicate analyses of alkali basalts indicate precision of 3–6% for Sc, Cr, La, Eu, Tb, and 6–10% for other elements. Accuracy indicated by standard rock data in Frey et al. (1974)

[b] Analyses by B. Schroeder, W.H.O.I. See Schroeder et al. (in press) for details on analytical methods

[c] M.I.T. lab, analytical methods in Hart and Brooks (1977)

[d] Measured ratio with 2σ errors, all ratios relative to Eimer and Amend value of 0.70800

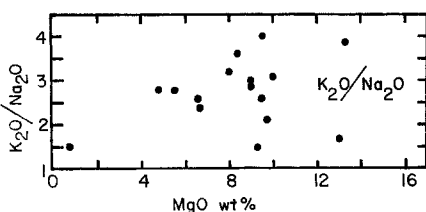[e] Calculated initial ratio, see text for discussion

Fig. 4. Plot of K_2O/Na_2O versus MgO for Navajo minettes. Data from Ehrenberg (1977), Nicholls (1969), Roden and Smith (1979), Williams (1936)

ettes at Washington Pass (Ehrenberg 1977) and at Buell Park (Roden and Smith 1979) suggests that the compositional diversity of the minettes was established prior to the incorporation of these xenoliths in the upper mantle (see discussion in Roden and Smith 1979). In the previous study of the Buell Park center Roden and Smith (1979) evaluated a fractional crystallization model based on microprobe analyses of phenocrysts and whole rock analyses using a Wright and Doherty (1970) least squares model to explain the relation of minette varieties at Buell Park. Because of the high residuals for FeO and TiO_2 in the fractional crystallization model, they suggested that these lavas could only be related by varying amounts of partial melting or high pressure fractionation of phenocrysts plus some phases (e.g. magnetite) not present as phenocrysts. In these models the felsic minettes were treated as liquids; but this assumption must be qualified because abundant ultramafic and crustal xenoliths occur in the felsic minettes in a size range (to less than a mm in diameter) such that it was impossible to completely separate minette from xenoliths when preparing rock powders. Thus, an accidental component is included in the measured compositions of the felsic minettes. A further complication lies in the porphyritic texture of both mafic and felsic minette; thus whole rock compositions include crystals plus liquid, but an assumption in the fractional crystallization model is that the rock compositions represent liquids. This problem will lead to the deviation of model predictions from measured compositions, especially for compatible

Table 3. Partition coefficients

	Diopside	Apatite A	Apatite B	Olivine	Enstatite	Garnet	Phlogopite	Magnetite
Ce	0.096	9.2	17	0.010	0.009	0.02	0.034	0.03
Nd	0.18	11	21	(0.013)	(0.015)	0.09	0.032	0.04
Sm	0.26	11	21	0.015	0.022	0.22	0.031	0.05
Dy	0.31	9.8	17	(0.022)	(0.09)	1.1	0.030	0.11
Er	0.23	7.5	14	0.027	0.13	2.2	0.034	0.12
Yb	0.23	4.1	9.4	0.033	0.17	4.0	0.042	0.11
Ba	0.001	1	1	–	–	–	1.1	–
Sr	0.1	2	2	–	–	–	0.1	–
Rb	0.002	–	–	–	–	–	3.1	–
Sc	3.3	–	–	0.3	1	28	1	1
Cr	3	–	–	1	1.5	18	3	100
Ni	3	–	–	10	2	5	3	20
V	1	–	–	–	–	–	1	20
References	1, 2	3, 12	4, 12	5, 2	6, 2	7, 2	8, 9, 10, 11	1, 2

Values in parentheses are interpolated

References:
1. Kay and Gast 1973
2. Values are consistent with data in Irving 1978
3. Irving 1978
4. Nagasawa and Schnetzler 1971
5. McKay and Weill 1975
6. Weill and McKay 1975

7. Frey et al. 1978
8. Schnetzler and Philpotts 1970
9. Philpotts and Schnetzler 1970
10. Dawson and Smith 1975
11. Phlogopite K_d^{Cr} from coexisting phlogopite and glass, Roden 1977
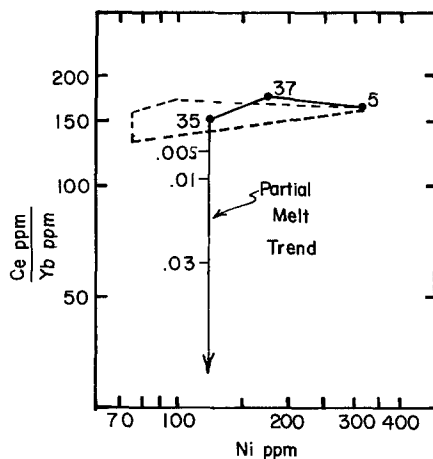12. Dasch 1969

Fig. 5. Ce/Yb plotted as a function of Ni ppm for samples BPR-5, BP-37, and BP-35 (connected by the solid line). *Straight line* labeled *"partial melt trend"* shows expected values for increasing amounts of melting assuming that (1) BP-35 represents the smallest degree of melting of the minettes, (2) the source mineralogy specified in the text, and (3) nonmodal batch melting. Rapid change in Ce/Yb ratio in melt as melting increases is emphasized by numbers along partial melt trend which indicate fraction of melt if BP-35 is a 0.1% melt of source. Area outlined by *dashed line* shows expected variation of Ce/Yb with Ni during crystal fractionation assuming that the parent melt had a Ce/Yb ratio and Ni content similar to that of BPR-5, and that phases fractionated in the proportions specified in the text. In the latter model, a region rather than a line is plotted because two sets of apatite coefficients were used in the crystal fractionation model

elements. Hence, the model can only be used in a qualitative sense.

The trace elements Ce, Yb, Sc, Cr, Ni, and the Ce/Yb ratio were used to discriminate between fractional crystallization and partial melting models as the explanation for the minette compositional diversity. Ce and Yb are typically incompatible elements

during crystal fractionation while Cr, Sc, and Ni are compatible. Fractional crystallization was modelled with the partition coefficients (simple weight ratios) in Table 3 and a Rayleigh fractionation equation:

$$C^1/C^0 = F^{D-1}$$

where C^1 is the concentration of the trace element in the liquid, C^0 is the original concentration of the trace element in the liquid, F is the fraction of liquid remaining, and D is the bulk distribution coefficient. Mineral proportions were fixed by the crystal fractionation model developed by Roden and Smith (1979): 49% diopside + 32% phlogopite + 8.5% magnetite + 5.5% apatite + 4.4% olivine subtracted from ring dike sample BPR-5 yields felsic minette BP-37. Further minor fractionation of diopside, phlogopite, apatite, and magnetite from BP-37 yields felsic minette BP-35. The fraction of liquid, F, for the two steps was 0.63 and 0.87 respectively. To model partial melting, a garnet peridotite source was used: 10% garnet, 10% clinopyroxene, 25% orthopyroxene, and 55% olivine, which melted in the proportions: 45% garnet, 45% clinopyroxene, 5% olivine, and 5% orthopyroxene, according to the nonmodal batch melting Equation 15 of Shaw (1970). Partition coefficients used are listed in Table 3. The results of both models are displayed in Figs. 5 and 6. Note that minette sample BP-69 is not included in these models; this sample has a high water content and has probably been altered (Roden and Smith 1979).

During partial melting the Ce/Yb ratio of the melt decreases rapidly with increased melting while the concentrations of the compatible elements Yb (Yb is compatible because of residual garnet), Sc, Cr, and Ni remain relatively constant. The decrease in Ce/Yb ratio results primarily from the dilution of the incompatible element Ce with increased melting while Yb concentration remains essentially constant because garnet is residual. Beyond 10% melting Sc, Yb, and Cr increase in the melt because residual garnet is being exhausted while Ni concentration in the melt remains near constant beyond 20% melting because of the persistence of olivine in the residuum. The high and
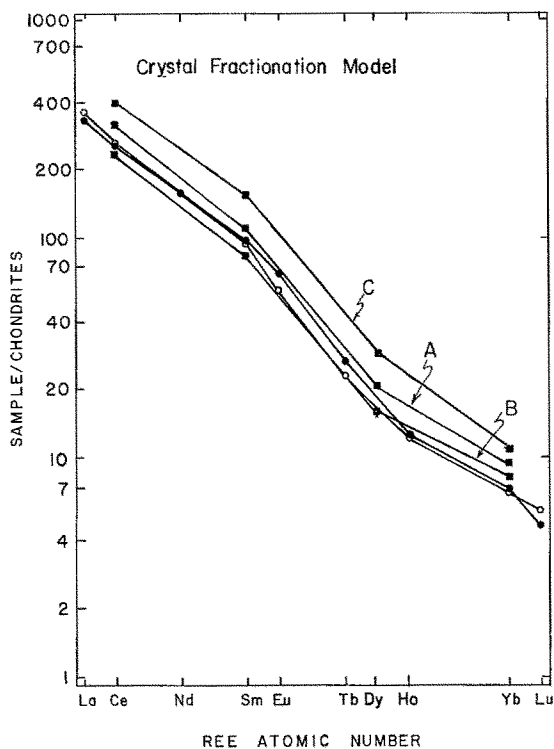
Fig. 6. Crystal fractionation model for the REE in the minettes compared to the observed REE concentrations of a ring dike sample (●) and felsic minette BP-37 (○). Phase proportions are specified in the text and the partition coefficients used are shown in Table 3. The three model curves (■) represent liquids derived by crystal fractionation from the ring dike minette; they differ with respect to apatite partition coefficients used: (A)=partition coefficients of Irving 1978, (B)=partition coefficients of Nagasawa and Schnetzler 1971, (C)=no apatite fractionation

Table 4. Discrepancies in crystal fractionation model

		°C	STEP 1	STEP 2
F		1	0.63	0.63 × 0.87
Corresponding minette		BPR-5/6	BP-37	BP-35
Cr ppm	model	412	4	1
	observed	412	234	154
Ni ppm	model	322	61	39
	observed	322	176	123
V ppm	model	193	97	78
	observed	193	132	100
Ba ppm	model	2,165	2,815	2,980
	observed	2,165	2,270	2,280
Sr ppm	model	1,338	1,870	
	observed	1,338	1,209	
Rb ppm	model	115	113	105
	observed	115	200	214

relatively constant Ce/Yb ratio of the minettes (Fig. 3) restricts them to similar degrees of partial melting (Fig. 5) and the high Ce concentration of the minettes restricts them to low percentages of partial melting. Over such a small range of melting the compatible elements Sc and Ni will not be fractionated. Hence, the fractionation of compatible elements combined with the high and near constant Ce concentration and Ce/Yb ratio of the minettes cannot be simply explained by varying amounts of partial melting (Fig. 5).

In contrast to the partial melting model, fractional crystallization can simultaneously account for the rapid decrease of the compatible elements and the behavior of the REE (Fig. 5). Sc, Cr, and Ni decrease rapidly during crystal fractionation because of the high K_d values diopside, phlogopite, olivine, and magnetite have for these elements. Normally, the REE would be expected to increase in the residual liquid during crystal fractionation while the Ce/Yb ratio remained nearly constant. In the case of the minette model, however, apatite acts to buffer the REE concentrations. Note that two sets of apatite partition coefficients for the REE were used in the model (Fig. 6) and the two model REE curves (A, B, Fig. 6) nearly bracket the observed REE curve of felsic minette BP-37 when the REE concentrations in BPR-5 are used as the model parent. Note further, that without the fractionation of apatite, the model daughter liquid (C, Fig. 6) has considerably higher REE concentrations than that observed in BP-37. Fractionation of apatite is further supported by a decrease of P_2O_5 from mafic to felsic minette (Fig. 3), by the occurrence of apatite in cognate phlogo-

pite-diopside xenoliths (Ehrenberg 1978), and by the observation that apatite is stable in the melting interval of a Leucite Hills madupite to pressures above 25 kb (Barton and Hamilton 1979).

A larger K_d^{Ni} for olivine, such as 20 instead of 10, may be more appropriate for the Mg-poor felsic minettes (Hart and Davis 1978). If this larger K_d^{Ni} is used for the felsic minettes in the equilibrium melting model, then the liquid contains 190 to 210 ppm Ni over a range of melting of 0.1% to 20%. This lower Ni concentration in the model liquids is in reasonable agreement with the observed concentration (176 ppm) of BP-37. However textural evidence suggests that the felsic minettes were not in equilibrium with olivine. There is no evidence for olivine phenocrysts in the felsic minettes and peridotite nodules are surrounded in the felsic minettes by reaction coronas of phlogopite+diopside±magnetite (Roden 1977; Ehrenberg 1978). This lack of olivine in felsic differentiates is to be expected during fractional crystallization if the reaction relationship with falling temperature between olivine and potassic magma found for a Leucite Hills madupite (Barton and Hamilton 1979) is applicable to the Navajo rocks. Thus, it is maintained that fractional crystallization is the best explanation for the fractionation of compatible elements and constant Ce/Yb ratio of minettes at Buell Park.

An interesting observation is that elements which are normally incompatible (REE, Rb, Ba, Sr, Th, P, Nb, Ta) during the differentiation of basalts behave in diverse ways in the minettes. Only Rb and Th behave incompatibly (Table 2) while the REE, Ba, and Sr remain nearly constant from mafic to felsic minette. Three of the elements P, Nb, and Ta, behave compatibly and decrease from mafic to felsic minette. The anomalous behaviour of normally incompatible elements probably reflects the fractionation of large-ion-lithophile-element-rich phlogopite and apatite.

In detail, for many trace elements (e.g. Cr, Ni, Ba, Sr, Rb) concentrations in the model liquids of the crystal fractionation model do not match the observed trends (Table 4). If the model is valid then this discrepancy likely results for several reasons. Modelling of Cr and Ni is complicated by the abundance of xenocrysts from and xenoliths of ultramafic nodules in the felsic minettes. Ultramafic xenoliths are extremely rich in Cr and Ni, and thus, measured Cr and Ni abundances in the felsic minettes will be significantly higher then the real concentrations of the magmas. In addition, Cr and Ni along with V are all sensitive to the fraction of magnetite in the cumulate because of the

large partition coefficients that magnetite has for these elements (Table 3). Neither the magnetite partition coefficients nor the fraction of magnetite in the model are well known. The observed deviations from the model for Cr, Ni, and V (Table 4) are attributed to these problems. Modelling for Ba is complicated by the evidence of high BaO concentrations, 0.60 wt. % (Nicholls 1969) in phlogopite phenocrysts in a Buell Park felsic minette. A larger K_d^{Ba} for phlogopite would be more consistent with the measured BaO in the phlogopite phenocryst and would bring the model into better agreement with the observed concentrations in the minettes. Poor knowledge of partition coefficients for phlogopite and apatite also affect the modelling of Rb and Sr: phlogopite fractionation will have a major effect on Rb concentrations in derivative liquids, and apatite fractionation may have a similar effect on Sr (a more detailed description of these problems is available from the writer on request).

An intriguing observation is the decrease of Nb and Ta concentrations with increasing differentiation of the minettes. Mineral partition coefficients are unknown, but Nb and Ta normally behave coherently and incompatibly during magmatic processes (Goldschmidt 1954). Ta and Nb substitute for Ti in silicate and oxide minerals, and are concentrated in titaniferous minerals in igneous rocks (Goldschmidt 1954; Parker and Fleischer 1968). Thus, fractionation of a titanium-rich mineral could explain the decrease in Nb and Ta from mafic to felsic minette. The bulk distribution coefficients for Nb and Ta can be estimated by solving for D in the Rayleigh fractionation equation knowing that C^1/C^0 is specified by the abundances of Nb and Ta in the minettes and that F is specified by the fractionation model based on the major elements. The calculated bulk distribution coefficients range from 2 to 4 for Nb and 2 to 3 for Ta for the two steps of the fractionation model. Ilmenite, titanomagnetite, and titaniferous phlogopite all occur as phenocryst or groundmass phases in the Buell Park minettes (Roden and Smith 1979). Ilmenite occurs in the groundmass of the mafic ring dike, but the published partition coefficient for Nb in ilmenite, $K_d^{Nb} = 0.8$ (McCallum and Charette 1978), is too low to explain the calculated bulk distribution coefficient for Nb. Titanomagnetite is not a sink for Nb and Ta in igneous rocks (Parker and Fleischer 1968). Phlogopite or biotite contain significant amounts of Ta and Nb in igneous rocks, but in general have lower concentrations of these elements than coexisting ilmenite (Parker and Fleischer 1968). However, the very high TiO_2 contents, up to 11.3% (Roden and Smith 1979), of the phlogopite phenocrysts at Buell Park suggests that this mineral could contain abnormally high concentrations of Nb and Ta, and that fractionation of phlogopite could explain the decrease of Nb and Ta from mafic to felsic minette.

In summary, crystal fractionation best explains the decrease of compatible trace elements and the buffering or slow increase of incompatible trace elements from mafic to felsic minettes at Buell Park. The signature of this simple process has been somewhat obscured by the mechanical incorporation of Cr- and Ni-rich peridotite nodules. Trace element evidence cannot completely eliminate the possibility that the minettes are related by varying amounts of partial melting, but this explanation appears unlikely.

3. Relation of Minette Compositional Types: Sr Isotopic Evidence

The heterogeneity of calculated initial $^{87}Sr/^{86}Sr$ ratios (Table 2) suggests that another process in addition to fractional crystallization was important at Buell Park. Note that the initial ratios

reported here are lower than the initial $^{87}Sr/^{86}Sr$ ratios, 0.7077 and 0.7075, that Powell and Bell (1970) reported for a felsic and mafic minette from Buell Park. Direct comparison between the data sets is impossible because Powell and Bell (1970) do not report a standard analysis nor do they describe the age correction they applied to the minette analyses. The heterogeneity of the initial ratios reported here is marginally consistent with the lower analytical precision reported in Powell and Bell (1970).

The observed heterogeneity of the whole rock initial ratios could be explained by either crustal contamination or source heterogeneity. The latter hypothesis cannot explain the lack of correspondence between the calculated initial ratios of host minette and separated phlogopite (Table 2). The hypothesis of crustal contamination is supported by the widespread occurrence of crustal xenoliths in the minettes of the Navajo field (Williams 1936), and their common occurrence in the felsic minettes at Buell Park (Roden and Smith 1979). However, the minettes have high Sr concentrations relative to most crustal rocks, and thus are relatively insensitive to contamination by common crustal materials. However, Taylor (1980) argued that even high Sr magmas are susceptible to contamination as evidenced by a positive correlation between oxygen and strontium isotopic ratios in some volcanic rocks. As one example of a contaminated magma series, he chose the Sr-rich (500–2,000 ppm) high-K series from Roccamonfina volcano. The geochemistry of this magma series is similar to that of the Navajo minettes. Further permissive evidence at Buell Park for crustal contamination includes the small volume of magma erupted and the occurrence of rare, large biotite crystals in some thin sections of the Buell Park felsic minettes. These biotites were initially identified by their distinct pleochroism and later, microprobe analyses of several grains from a felsic Buell Park minette showed that the biotites have Mg/Fe ratios between 0.84 and 0.96 (Roden, unpublished data); no micas with Mg/Fe ratios intermediate between these biotites and the phlogopite phenocrysts exist at Buell Park (Roden and Smith 1979). Thus, these biotites are likely xenocrysts, and their presence implies that some crustal material was disaggregated during incorporation in the minettes. The presence of a small amount of radiogenic biotite derived from crustal rocks in the phlogopite separate can explain the high $^{87}Sr/^{86}Sr$ ratio of the phlogopite relative to the bulk rock. Note, however, that the calculated initial $^{87}Sr/^{86}Sr$ ratio of BP-37 Mica is very sensitive to the age used; for example if the mica is 30 m.y. old then the calculated initial $^{87}Sr/^{86}Sr$ ratio of the mica is 0.70727 and that of the host rock is 0.70682. However, the age of this separate is well constrained by 6 K–Ar ages on this separate and 5 other micas from Buell Park and surrounding diatremes (Roden et al. 1979). These data also imply that any xenocrystal biotite was degassed upon incorporation in the minette magma. Based on the above arguments crustal contamination will be adopted as a working hypothesis to explain the heterogeneous initial $^{87}Sr/^{86}Sr$ ratios of the Buell Park minettes. Admittedly, this hypothesis cannot be proven until further isotopic data, especially oxygen isotopic data are gathered. And at least one field observation is at a variance with the contamination hypothesis: the occurrence of dense ultramafic xenoliths in the felsic minettes and their absence from the mafic minettes implies that differentiation occurred in the upper mantle and not in the crust.

The likelihood of crustal contamination invalidates the simple model Roden and Smith (1979) discussed which related the high initial $^{87}Sr/^{86}Sr$ ratios of the Navajo minettes to source characteristics. The lowest initial ratio, 0.70551, reported here must represent an upper limit to the $^{87}Sr/^{86}Sr$ ratio of the source

because of the assimilation problem. An isotopic survey of the mafic Navajo minettes is needed to ascertain how close this lowest initial $^{87}Sr/^{86}Sr$ ratio is to that of the source, and whether the source material for these unusual lavas was isotopically uniform throughout the region.

4. Nature of the Kimberlitic Tuff

Dawson (1967a) defined kimberlites as serpentinized and carbonated mica peridotites which contain ultramafic nodules. An important petrographic feature is the occurrence of *Phenocrysts* of olivine, garnet, pyroxenes, and most significantly, mica, ilmenite, and amphibole in a fine grained groundmass. Dawson (1967b) also stressed the high K_2O, P_2O_5, TiO_2 contents, and the high K/Na ratio of kimberlites relative to other peridotites. The green, serpentine-rich tuffs of the Navajo volcanic field initially were called kimberlite (Allen and Balk 1954) because of their field relations and peridotitic mineralogy. Because "kimberlite" has been applied to these tuffs, the Navajo field has been cited in the literature as an example of a kimberlite-potassic lamprophyre association. However, petrographically the Navajo "kimberlites" differ from true kimberlites in several ways: most peridotitic mineral grains are derived from the comminution of mantle-derived xenoliths and thus are not phenocrysts, there is no evidence that these tuffs were ever a true magma, and the tuffs lack the LIL-element-rich minerals such as phlogopite and perovskite which are typical of kimberlites (McGetchin and Silver 1972; Smith and Levy 1976; Smith 1977). The issue is somewhat confused because Aoki et al. (1972, 1976) argued that richterite-rich amphibole, titanochondrodite, and titanoclinohumite, which occur in the Buell Park tuffs, formed by crystallizing from a kimberlite magma. Smith (1977), on the other hand, replied that the compositions of discrete grains of these minerals overlapped compositions of these minerals in xenoliths at Green Knobs; hence it is probable that the discrete grains formed by comminution of rock fragments rather than as phenocrysts. The two published major element analyses of "kimberlite" from Buell Park (Schmitt et al. 1974; Allen and Balk 1954) support the contention that these tuffs are not kimberlitic because the tuff is depleted in TiO_2, K_2O, and P_2O_5 compared to typical kimberlites (Gurney and Ebrahim 1973; Dawson 1967b).

In order to further illuminate the problem of the nature of the kimberlitic tuffs, matrix from the Buell Park tuff, NBP4-17, was analyzed for trace elements and $^{87}Sr/^{86}Sr$ ratio (Table 2). This matrix material is light REE enriched (Fig. 2) relative to chondrites, and has high La, Ba, Rb, and Sr concentrations compared to other peridotites, but compared to kimberlites (e.g. Fesq et al. 1975) the Buell Park tuff has very low light REE, Rb, and Sr abundances. In spite of efforts taken to avoid xenoliths during sample preparation, the high $^{87}Sr/^{86}Sr$ ratio of the matrix (Table 2) suggests that a crustal component is present in the matrix. Thus, the high Rb, Ba, Sr, and light REE concentrations relative to most ultramafic rocks is likely due to the presence of this crustal component. The available chemical and petrographic data suggest that it is improper to apply "kimberlite" to the serpentine-rich tuffs of the Navajo volcanic field. For the remainder of this paper, these tuffs will be referred to as "serpentinized ultramafic microbreccias" (SUM; McGetchin and Silver 1972), and it is suggested that this term be used in the future when referring to the serpentine-rich tuffs of the Navajo country.

5. Petrogenesis: A Physical Model

Any physical model for the Buell Park rocks must explain the association in time and space of the SUM and the minettes

at Buell Park. McGetchin et al. (1973) hypothesized that the SUM of the northern diatremes were emplaced by a supercritical, volatile-rich phase. Observations at Buell Park and Green Knobs (Smith and Levy 1976) confirmed the hypothesis that the microbreccias were never a silicic melt and that they probably were deposited as a gas-solid mixture. Smith and Levy suggested that the volatiles in this system originated from CO_2 and H_2O liberated during the intrusion of hot minette magma into volatile-rich garnet peridotite. Alternatively, the components of the supercritical phase may have initially been in solution in the minette magma, i.e. possibly the explosive eruptions of the Navajo SUM correspond to the explosive eruptions suggested by Wyllie (1979) to result from a volatile-rich magma whose path during a near-adiabatic rise towards the surface intersected a solidus maximum in the peridotite-CO_2-H_2O system. In this case, the SUM are intrinsically related to the minettes as a supercritical phase which exsolved from freezing minette magma. Minette varieties exposed at the surface represent portions of a rising magma diapir (?) which did not undergo this catastrophic evolution of a supercritical fluid. As pointed out by Ehrenberg (1977) differentiation could occur during the rise of a small volume of initially homogeneous and potassic magma through a large volume of mantle wall rock. The felsic minettes correspond to the upper portion of this magma body which continuously encountered cooler wall rock, and lost heat: the consequence of this heat loss would be the plating of the conduit walls with crystallization products. The lower portion of this magma body, however, was protected from reaction with the heated wallrock by a zone of crystals formed by wallrock-minette reaction. Thus, the lower portion of the magma diapir lost less heat and differentiated less than the upper portion. The end result was a compositionally stratified diapir which is more differentiated at the top. Thus, the present association of mafic minette, felsic minette, and SUM, may reflect the differentiation of an initially homogeneous and mafic, potassic magma.

The model described above may explain the origin of the SUM and the relation of mafic and felsic minette at Buell Park and also at the Shiprock-Mitten Rock centers (Fig. 1; Ehrenberg 1977). However, felsic minettes at Sonsela Buttes and Washington Pass, because of their high MgO contents (Ehrenberg 1977) are distinct from the Buell Park and Mitten Rock felsic minettes. The geochemistry of these high MgO, felsic minettes cannot be explained by crystal fractionation alone (Ehrenberg 1977).

6. Petrogenesis: Nature of the Source Material

Ehrenberg (1979) found that the minerals of garnet peridotite xenoliths in minette from The Thumb last equilibrated in a narrow depth range near 130 km thereby requiring that the minettes originated from greater depths. Formation of the minette magma within the garnet stability field is consistent with the high Ce/Yb ratios (Kay and Gast 1973) of the minettes. These high Ce/Yb ratios indicate the important role of garnet as a residual phase during melting (Kay and Gast 1973). Kay and Gast suggested that the minettes formed by small percentages (less than 1%) of partial melting of a garnet peridotite source with a flat REE pattern relative to chondrites; however, the REE data do not constrain the source to have a chondritic REE pattern. If the minettes formed by greater than 1% partial melting then the source had to be enriched in the light REE relative to chondrites such as the source suggested by Frey et al. (1978) for a series of light REE enriched basalts from southeastern Australia. These ideas are further illustrated in Fig. 7 and
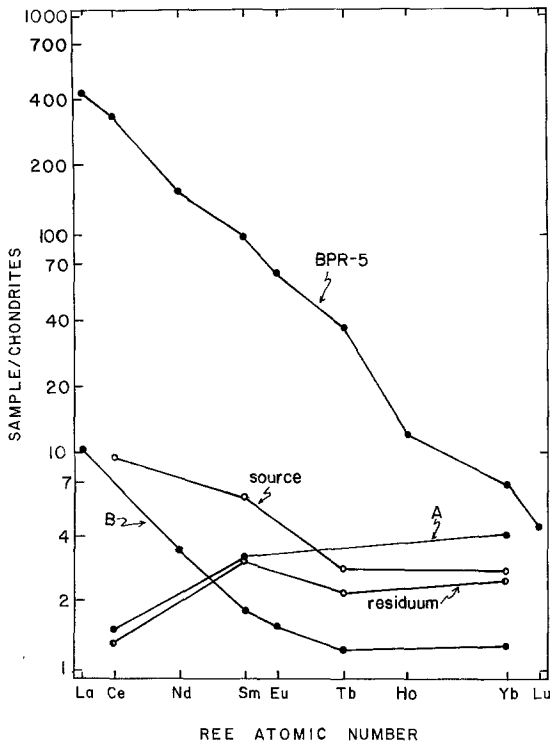
Fig. 8. P_2O_5 versus Ce diagram for primitive $(Mg/Mg+Fe^{2+} \geq 63$, $Ni > 100$ ppm) alkali basalts, basanites, and nephelinites (data obtainable from the writer on request). Data points include those of Frey et al. 1978, and Sun and Hanson 1975. These basalts are indicated by solid circles and fall near a line with $P_2O_5/Ce = 75$. The mafic Navajo minettes are indicated by *open circles* (data from Ehrenberg 1977, 1978; this paper) and fall to the right of this line. The minettes have relatively low P_2O_5/Ce ratios

Fig. 7. Source model for BPR-5 assuming 3% melting of a source with mineralogy specified in Table 4. Curve labelled "*BPR-5*" is the liquid composition, and the curves labelled "*source*" and "*residuum*" are the model source and residuum. *Curve A* is "*normal suboceanic mantle*" (White and Schilling 1978), *Curve B* is the upper limit to the REE concentrations in light REE enriched nodules from Victoria (Frey and Green 1974). See text for discussion

Table 5. Peridotite source model

	Diopside	Enstatite	Olivine	Garnet
Initial mode	0.10	0.25	0.55	0.10
Melt composition	0.45	0.10	0.10	0.45
Residuum mode after 3% melting	0.0892	0.2562	0.5655	0.0892

	Ce	Sm	Tb	Yb
Bulk partition coefficient, D_i	0.006	0.033	0.082	0.38
C_i^l ppm (BPR-5)	238	18.2	1.32	1.42
C_i^s ppm	1.45	0.61	0.11	0.54
C_i^0 ppm	8.54	1.13	0.14	0.57

Table 5 which were constructed using the following equations and assuming a nominal melting percentage of 3%:

$$D_i = C_i^s/C_i^l$$

$$C_i^0 = X_s(C_i^s) + (1 - X_s)(C_i^l)$$

where D_i is the bulk distribution coefficient for element i; C_i^s is the concentration of i in the solid residuum; C_i^l is the concentration of i in the melt, that is mafic minette BPR-5; C_i^0 is the original concentration of i in the source; and X_s is the weight fraction, 0.97, of the residuum in the solid-melt system. The model source for the minettes is light REE-enriched and has a chondrite-normalized REE pattern similar to light REE-enriched peridotite nodules from alkali basalts (e.g. Frey and Green
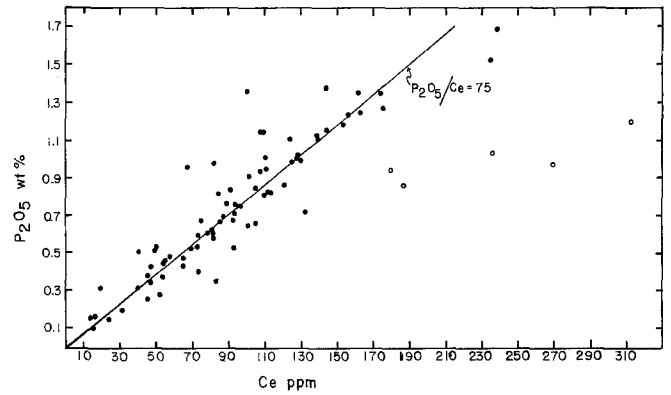
1974). These light REE-enriched nodules are probably samples of mantle enriched in incompatible elements relative to primitive mantle; i.e., the nodules are samples of what is called metasomatized mantle (e.g. Boettcher et al. 1979).

Several independent lines of evidence suggest that the source material for the minettes was metasomatized mantle relatively enriched in the light REE and other incompatible elements. Firstly, the presence of phlogopite and apatite as phenocrysts and microphenocrysts in the minettes and their important role during the differentiation of the minettes is consistent with their initial presence in the source. Phlogopite and apatite are commonly mineralogical indicators of metasomatized mantle (e.g. Boettcher al. 1979). Secondly, phlogopite-bearing garnet peridotite nodules occur in the Navajo field (Ehrenberg 1979) which indicates the existence of potassium-rich, i.e., metasomatized mantle in the region. Thirdly, mafic minettes of the Navajo field have low K/Rb, 156 to 387 (Ehrenberg 1977; Nicholls 1969; this paper), and low K/Ba, 13 to 30 (Ehrenberg 1978; Nicholls 1969; Kay and Gast 1973; this paper), relative to oceanic basalts (e.g. Hart 1976). These data suggest that either the source material was enriched in LIL-elements relative to oceanic mantle, or that these elements did not behave incompatibly during melting, that is, a LIL-element-rich phase such as phlogopite was residual during melting. Lastly, the low P_2O_5/Ce ratios of the mafic Navajo minettes (Fig. 8) indicates that they may have formed in equilibrium with residual apatite or that they formed from a source enriched in Ce relative to P. Most primitive alkali basalts, basanites, and nephelinites have P_2O_5 ratios of 75 ± 15 which probably reflects a uniform P_2O_5/Ce ratio in the source for these basalts (Sun and Hanson 1975; Frey et al. 1980). In contrast, the mafic minettes $(MgO/MgO + FeO \geq 68$; $Ni > 200$ ppm) have P_2O_5/Ce ratios ranging from 36 to 52 and lie distinctly off the main trend in Fig. 10. These low P_2O_5/Ce ratios are consistent with either residual apatite controlling the P_2O_5/Ce ratio of the melt or early apatite fractionation. Alternatively, if P and Ce behaved incompatibly during melting then the low P_2O_5/Ce ratios of the minettes indicates that their source was distinct in P_2O_5/Ce ratio relative to the source for other basalts. Beswick and Carmichael (1979) noted that potassic basalts commonly have lower P_2O_5/Ce ratios than other basalts.

Insofar as the Navajo minettes share with the rocks of the ultrapotassic series their peculiar geochemical characteristics, hy-

potheses regarding the origin of the minettes have important implications for the origin of other members of the ultrapotassic series. The implications are particularly important because of the documented occurrence of mantle-derived xenoliths in the minettes and associated SUM. Ultramafic xenoliths occur in at least two other potassic volcanic fields: Chino Valley, Arizona (Arculus and Smith 1979) and Leucite Hills (Ogden et al. 1978). The implication is that the mafic, potassic lavas of the ultrapotassic series formed by partial melting in the upper mantle of regions intrinsically rich in K_2O. During transport to the surface these magmas may react with wallrock and differentiate to a SiO_2-rich liquid rich in K_2O and Na_2O. Small volumes of potassic and magnesian lavas similar in composition to the Navajo minettes were erupted in widely separated explosive volcanic fields during the Tertiary period in the western United States. The positions of these volcanic fields are independent of the regional structural style; for example, they occur on the Colorado Plateau (Navajo field), southwestern margin of the Colorado Plateau (Chino Valley), southern Rocky Mountains (Spanish Peaks, Jahn et al. 1979), Great Plains (Two Buttes, Krieger and Thornton 1976), Wyoming Basin (Leucite Hills, Carmichael 1967), Sierra Nevada (San Joaquin-Kings, Moore and Dodge 1980), and the eastern edge of the northern Rocky Mountains (Highwood and Bearpaw Mountains, Hearn et al. 1977). Thus, the location of potassic volcanism appears to be independent of regional crustal structure, although the location of eruptive centers was controlled by local structure. These potassic volcanic fields are most likely the expression of partial melting of LIL-element-enriched, metasomatized peridotite which was common to several regions of the subcontinental mantle beneath the western United States during the Tertiary period.

Conclusions

Based on trace element and Sr isotopic studies of the Buell Park rocks the following conclusions are reached:

(1) The felsic minettes formed by crystal fractionation from mafic minette in the upper mantle;

(2) At Buell Park felsic minette assimilated some crustal rocks;

(3) The kimberlite at Buell Park lacks the high concentrations of incompatible trace elements of other kimberlites; it is most likely a mixture of comminuted mantle wall rock and crustal material. These rocks should be no longer called kimberlite; "serpentinized ultramafic microbreccias" (SUM) is a more appropriate term. These SUM may be genetically related to the minettes as a vapor phase which exsolved from freezing minette magma in the upper mantle;

(4) The most likely origin of the Navajo minettes is by a small amount of melting of a metasomatized garnet peridotite.

Appendix. Sample descriptions

BPR-5

Ring dike sample (analysis in Table 1), lamprophyric texture, phenocrysts of diopside (5%) with aegirine-rich rims, altered olivine (10%),

and sparse, titaniferous (to 11 wt. % TiO_2) phlogopite. Matrix of aegirine-rich diopside, sanidine, phlogopite, analcime, ilmenite, and magnetite. Xenolith-free, but rare pyroxene phenocrysts have green, salite cores interpreted as xenocrysts (Roden and Smith 1979).

BPR-6

Ring dike sample, texture is similar to BPR-5, but diopside phenocrysts (11%) are more common than fresh, zoned (Fo_{86} core to Fo_{78} rim) olivine (5%). Xenolith-free, but salite-cored pyroxenes are sparsely distributed. Chemically BRP-6 is essentially identical to BPR-5 except that it contains more Na_2O (2.1% versus 1.3%) and less K_2O (4.9% versus 5.2%).

BP-37

Flow banded minette bomb from Buell Mountain (Table 1). More SiO_2-rich and MgO-poor than the ring dike samples (Table 1). Olivine absent. Phlogopite (8%) and diopside (11%) phenocrysts in a devitrified matrix of sanidine, oxides, apatite, and mesostasis. Xenoliths abundant and dominated by oxidized ultramafic rocks.

BP-37 Mica

Phlogopite phenocryst separate from sample BP-37. This phlogopite has a K-Ar age of 25.2 ± 0.4 million years (Roden et al. 1979).

BP-35

Felsic minette (Table 1) from a plug of minette which occupies the center of the vent on Buell Mountain. Apparently, the youngest minette unit in the vent area and also the poorest in MgO (Table 1). Phenocrysts of diopside (11%), phlogopite (5%), and minor sanidine in a trachytic matrix of sanidine, diopside, mica, and minor oxides, quartz, and apatite. Xenoliths common (5%) and mostly ultramafic, but crustal xenoliths also occur.

BP-69

Minette clast from layered kimberlitic tuff on Buell Mountain. This sample forms part of the evidence for overlap of minette and kimberlite eruptions and represents the oldest minette unit on Buell Mountain. Phenocrysts of phlogopite (4%), diopside (6%), and sanidine (3%) in dark grey mesostasis, largely clay after glass. This sample is notable for oval areas now filled with serpentine (?) which resemble euhedral olivine. The composition of this sample is also unique: it is quite siliceous (55.5% SiO_2) but unlike the other felsic minettes, it is also quite magnesian (9.2% MgO).

NBP4-17

Kimberlitic tuff collected from prominent knob of kimberlitic tuff in the eastern part of Buell Park. This sample is a breccia on all scales, but unlike many other Navajo kimberlites, the fragments are dominantly ultramafic in composition. The rock consists mainly of serpentinized ultramafic and other rock fragments, plus xenocrysts of olivine and pyroxene and pseudomorphs after these minerals in a green, serpentine-rich matrix.

References

Allegre CJ, Minster JF (1978) Quantitative models of trace element behavior in magmatic processes. Earth Planet Sci Lett 38:1–25

Allen JE, Balk R (1954) Mineral resources of Fort Defiance and Tohatchi quadrangles, Arizona and New Mexico. NM, Bur Mines Mineral Resour, Bull 36:140 p

Aoki K, Fodor RV, Keil K, Dowty E (1972) Tremolite with high richterite-molecule content in kimberlite from Buell Park, Arizona. Am Mineral 57:1889–1893

Aoki K, Fujino K, Akaogi M (1976) Titanochondrodite and titanoclinohumite derived from the upper mantle in the Buell Park kimberlite, Arizona, USA. Contrib Mineral Petrol 56:243–253

Arculus RJ, Smith D (1979) Ecologite, pyroxenite, and amphibolite inclusions in the Sullivan Buttes latite, Chino Valley, Yavapai

County, Arizona. In: Boyd FR, Meyer HOA (eds) The mantle sample: Inclusions in kimberlites and other volcanics. Am Geophys Union, Washington, pp 309–317

Barton M, Hamilton DL (1979) The melting relationships of a madupite from the Leucite Hills, Wyoming, to 30 Kb. Contrib Mineral Petrol 69:133–142

Bell K, Powell JL (1969) Strontium isotopic studies of alkalic rocks: the potasisum-rich lavas of the Birunga and Toro-Ankole regions, east and central equatorial Africa. J Petrol 10:536–572

Beswick AE, Carmichael ISE (1978) Constraints on mantle source compositions imposed by phosphorous and the rare-earth elements. Contrib Mineral Petrol 67:317–330

Boettcher AL, O'Neil JR, Windom KE, Stewart DC, Wilshire HG (1979) Metasomatism of the upper mantle and the genesis of kimberlites and alkali basalts. In: Boyd FR, Meyer HOA (eds) The mantle sample: Inclusions in kimberlites and other volcanics. Am Geophys Union, Washington, pp 173–182

Carmichael ISE (1967) The mineralogy and petrology of the volcanic rocks from the Leucite Hills, Wyoming. Contrib Mineral Petrol 15:24–66

Carmichael ISE, Turner FJ, Verhoogen J (1974) Igneous petrology. McGraw-Hill Book Co, New York, 739 p

Clarke DB, O'Hara MJ (1979) Nickel and the existence of high-MgO liquids in nature. Earth Planet Sci Lett 44:153–158

Dasch EJ (1969) Strontium isotope disequilibrium in a porphyritic alkali basalt and its bearing on magmatic processes. J Geophys Res 74:560–565

Dawson JB (1967a) A review of the geology of kimberlite. In: Wyllie PJ (ed) Ultramafic and related rocks. J Wiley and Sons, New York, pp 241–251

Dawson JB (1967b) Geochemistry and origin of kimberlite. In: Wyllie PJ (ed) Ultramafic and related rocks. J Wiley and Sons, New York, pp 269–278

Dawson JB, Smith JV (1975) Occurrence of diamond in a mica-garnet lherzolite xenolith from kimberlite. Nature 254:580–581

Ehrenberg SN (1977) The Washington Pass volcanic center: evolution and eruption of minette magmas of the Navajo volcanic field. Extended Abstracts, 2nd Int Kimberlite Conf, Santa Fe

Ehrenberg SN (1978) Petrology of potassic volcanic rocks and ultramafic xenoliths from the Navajo volcanic field, New Mexico and Arizona. Unpubl PhD thesis, UCLA, 259 p

Ehrenberg SN (1979a) Garnetiferous ultramafic inclusions in minette from the Navajo volcanic field. In: Boyd FR, Meyer HOA (eds) The mantle sample: Inclusions in kimberlites and other volcanics. Am Geophys Union, Washington, pp 330–344

Fesq HW, Kable EJD, Gurney JJ (1975) Aspects of the geochemistry of kimberlites from the Premier Mine and other selected South African occurrences with particular reference to the rare earth elements. Phys Chem Earth 9:687–707

Frey FA, Haskin MA, Poetz J, Haskin LA (1968) Rare earth abundances in some basic rocks. J Geophys Res 73:6085–6098

Frey FA, Green DH (1974) The mineralogy, geochemistry and origin of lherzolite inclusions in Victorian basanites. Geochim Cosmochim Acta 38:1023–1059

Frey FA, Bryan WB, Thompson G (1974) Atlantic Ocean floor: geochemistry and petrology of basalts from Legs 2 and 3 of the Deep Sea Drilling Project. J Geophys Res 79:5507–5527

Frey FA, Green DH, Roy S (1978) Integrated models of basalt petrogenesis: a study of quartz tholeiites to olivine melilitites from southeastern Australia utilizing geochemical and experimental petrological data. J Petrol 19:463–519

Frey FA, Roden MF, Zindler A (1980) Constraints on mantle source compositions imposed by phosphorus and the rare-earth elements: critical comments on the paper by AE Beswick and ISE Carmichael. Contrib Mineral Petrol 75:165–173

Goldschmidt VM (1954) Geochemistry. Clarendon Press, Oxford, 730 p

Gurney JJ, Ebrahim S (1973) Chemical composition of Lesotho kimberlites. In: Nixon PH (ed) Lesotho kimberlites, Lesotho National Development Corporation, Maseru, pp 280–284

Hart SR (1976) LIL-element geochemistry, Leg 34 basalts. In: Yeats RS, Hart SR (eds) Initial Reports of the Deep Sea Drilling Project, vol 34, US Government Printing Office, Washington, pp 283–288

Hart SR, Brooks C (1977) The geochemistry and evolution of early Precambrian mantle. Contrib Mineral Petrol 61:109–128

Hart SR, Davis KE (1978) Nickel partitioning between olivine and silicate melt. Earth Planet Sci Lett 40:203–219

Hearn BC, Marvin RF, Zartman RE, Naeser CW (1977) Geochronology of igneous activity in north-central Montana alkalic province. Geol Soc Am Abstr Progr 9:432

Irving AJ (1978) A review of experimental studies of crystal/liquid trace element partitioning. Geochim Cosmochim Acta 42:743–770

Jahn B, Sun SS, Nesbitt RW (1979) REE distribution and petrogenesis of the Spanish Peaks igneous complex, Colorado. Contrib Mineral Petrol 70:281–298

Kay RW, Gast PW (1973) The rare earth content and origin of alkali-rich basalts. J Geol 81:653–682

Krieger EW, Thornton CP (1976) Geology and petrology of the Two Buttes intrusion, southeast Colorado. Geol Soc Am Abst Progr 8:596–597

McCallum IS, Charette MP (1978) Zr and Nb partition coefficients: implications for the genesis of mare basalts, KREEP and sea floor basalts. Geochim Cosmochim Acta 42:859–870

McGetchin TR, Silver LT (1972) A crustal-upper mantle model for the Colorado Plateau based on observations of crystalline rock fragments in the Moses Rock dike. J Geophys Res 77:7022–7037

McGetchin TR, Nikhanj YS, Chodos AA (1973) Carbonatite-kimberlite relations in the Cane Valley diatreme, San Juan County, Utah. J Geophys Res 78:1854–1869

McKay GA, Weill DF (1976) Petrogenesis of KREEP. Proc Seventh Lunar Sci Conf: 2427–2447

Moore JG, Dodge FCW (1980) Late Cenozoic volcanic rocks of the sourthern Sierra Nevada, California: I. Geology and petrology: summary. Geol Soc Am Bull Part I, 91:515–518

Naeser CW (1971) Geochronology of the Navajo-Hopi diatremes. J Geophys Res 76:4978–4985

Nagasawa H, Schnetzler CC (1971) Partitioning of rare earth, alkali, and alkaline earth elements between phenocrysts and acidic igneous magma. Geochim Cosmochim Acta 35:953–968

Nicholls J (1969) Studies of the volcanic petrology of the Navajo-Hopi area, Arizona. Unpub PhD thesis, U Calif Berkeley 107 p

Ogden PR, Sperr JT, Gunter WD (1978) Morphology of a recent ultrapotassic volcanic field, Leucite Hills, southwestern Wyoming. Geol Soc Am Abstr Progr 10:140

Parker RL, Fleischer M (1968) Geochemistry of niobium and tantalum. US Geol Surv Prof Pap 611:1–43

Philpotts JA, Schnetzler CC (1970) Phenocryst-matrix partition coefficients for K, Rb, Sr, and Ba with applications to anorthosite and basalt genesis. Geochim Cosmochim Acta 34:307–322

Powell JL, Bell K (1970) Strontium isotopic studies of alkalic rocks: localities from Australia, Spain, and the western United States. Contrib Mineral Petrol 27:1–10

Roden MF (1977) Field geology and petrology of the minette diatreme at Buell Park, Apache County, Arizona. Unpubl MA thesis, U Texas Austin, 148 p

Roden MF, Smith D (1979) Field geology, chemistry and petrology of Buell Park minette diatreme, Apache County, Arizona. In: Boyd FR, Meyer HOA (eds) Kimberlites, diatremes, and diamonds: Their geology, petrology, and geochemistry. Am Geophys Union, Washington, pp 364–381

Roden MF, Smith D, McDowell FW (1979) Age and extent of potassic volcanism on the Colorado Plateau. Earth Planet Sci Lett 43:279–284

Roeder PL, Emslie RF (1970) Olivine-liquid equilibrium. Contrib Mineral Petrol 29:275–289

Schmitt HH, Swann GA, Smith D (1974) The Buell Park kimberlite pipe, northeastern Arizona. In: Karlstrom TNV, Swann GA, Eastwood RL (eds) Geology of Northern Arizona. Northern Arizona University, Flagstaff, Arizona, pp 672–698

Schnetzler CC, Philpotts JA (1970) Partition coefficients of rare earth elements between igneous matrix material and rock-forming-mineral phenocrysts: II. Geochim Cosmochin Acta 34:331–340

Schroeder B, Thompson G, Sulanowska M, Ludden JN (in press) Analysis of geologic materials using an automated X-ray fluorescence system. X-Ray Spectrom

Shaw DM (1970) Trace element fractionation during anatexis. Geochim Cosmochim Acta 34:237–243

Smith D (1977) Titanochondrodite and titanoclinohumite derived from the upper mantle in the Buell Park kimberlite, Arizona, USA, a discussion. Contrib Mineral Petrol 61:213–215

Smith D, Levy S (1976) Petrology of the Green Knobs diatreme and implications for the upper mantle below the Colorado Plateau. Earth Planet Sci Lett 29:107–125

Sun SS, Hanson GN (1975) Evolution of the mantle: geochemical evidence from alkali basalts. Geology 3:297–302

Taylor HP Jr (1980) The effects of assimilation of country rocks by magmas on $^{18}O/^{16}O$ and $^{87}SR/^{86}Sr$ systematics in igneous rocks. Earth Planet Sci Lett 47:243–254

Weill DF, McKay GA (1975) The partitioning of Mg, Fe, Sr, Ce, Sm, Eu, and Yb in lunar igneous systems and a possible origin of KREEP by equilibrium partial melting. Proc Sixth Lunar Sci Conf 1143–1158

White WW, Schilling JG (1978) The nature and origin of geochemical variation in Mid-Atlantic Ridge basalts from the central North Atlantic. Geochim Cosmochim Acta 42:1501–1516

Williams H (1936) Pliocene volcanoes of the Navajo-Hopi country. Geol Soc Am Bull 47:111–172

Wright TL, Doherty PC (1970) A linear programming and least squares computer method for solving petrologic mixing problems. Geol Soc Am Bull 81:1995–2008

Wyllie PJ (1979) Magmas and volatile components. Am Mineral 64:469–500